

Design, Fabrication & Testing of Spin-Valve Read Heads for High Density Recording

Ching Tsang, Robert E. Fontana, Tsann Lin*, D. E. Heim*,
Virgil S. Speriosu, Bruce A. Gurney & Mason L. Williams

IBM Research Division,
IBM Advanced Magnetic Recording Laboratory,
Almaden Research Center, 650 Harry Road, San Jose, CA 95120-6099
*IBM Storage Systems Division

ABSTRACT— Spin-valve sensors of the type NiFe/Cu/Co have been designed for optimal biasing behavior and successfully incorporated into a gigabit-type shielded read head configuration with a read trackwidth of $2\mu\text{m}$, a read gap of $0.25\mu\text{m}$, and a MR sensor height of $1\mu\text{m}$. The spin-valve sensor had a structure of 100\AA NiFe/ 25\AA Cu/ 22\AA Co/ 110\AA FeMn, and yielded a net spin-valve coefficient of $\sim 3.5\%$ at the completion of head processing. Uniform field testing of the read heads after wafer fabrication and lapping showed quiet and stable spin-valve response with near optimal bias performance. Recording tests of the read heads at a head-disk clearance of $1.5\mu\text{m}$ showed linear, non-saturated signal response on a media with an areal moment as high as 1.25memu/cm^2 , yielding reasonably symmetrical signals with peak-to-peak amplitudes ranging from $\sim 750\mu\text{V}/\mu\text{m}$ to as high as $\sim 1000\mu\text{V}/\mu\text{m}$ of read trackwidth. Linear density rolloffs and microtrack profiles have also been studied, and results showed behaviors closely agreeing with design targets for high density recording operations.

I. INTRODUCTION

In the last several years, there has been increasing interest [1..9] in the study and development of a new type of thin film sensor that utilizes the recently discovered Giant Magnetoresistance (GMR) effect [1] instead of the conventional Anisotropic Magnetoresistance (AMR) effect [10,11]. In comparison to the AMR sensors, the GMR sensors are expected to deliver much larger sensitivities as well as output amplitudes, making them attractive for applications in future high performance magnetic recording systems. These GMR sensors are however also inherently more complicated [1..4] than the typical AMR sensors, often comprising multilayer configurations with layer thicknesses that must be accurately controlled at only tens of Angstroms. A commonly studied GMR system is the spin-valve sensor configuration [2] as shown schematically in Fig. 1. It consists of a ferromagnetic free layer and a ferromagnetic pinned layer separated from each other by a thin spacer layer. The magnetic moment of the pinned layer is typically fixed along the transverse direction by exchange coupling with an antiferromagnetic layer (e.g. FeMn), while the magnetic moment of the free layer is allowed to rotate in response to signal fields. The resultant spin-valve response is given by [3]

$$\Delta R \propto \cos(\theta_1 - \theta_2) \propto \sin \theta_1 \quad (1)$$

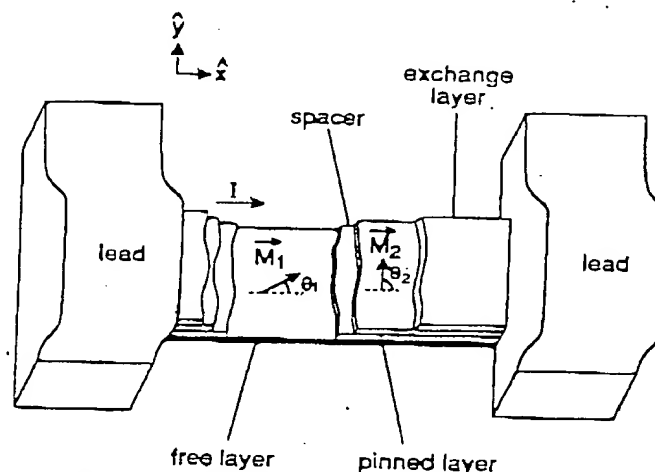


Fig. 1. Schematic of a spin-valve sensor (M : magnetic moment, θ : angle from the longitudinal direction).

where θ_1 and $\theta_2 (= \pi/2)$ represent the directions of free and pinned layer magnetic moments respectively (Fig. 1). If the uniaxial anisotropy hard-axis of the free layer is oriented along the transverse signal field direction, then the magnetic signal response is linear ($\sin \theta_1 \propto H$), yielding in turn a linear spin-valve sensor response through (1). This linear spin-valve sensor response is in contrast to the parabolic signal response of conventional MR sensors [10,11,12]. In a previous work [9], we have used micromagnetic modeling to study the magnetic behavior of unshielded and shielded spin-valve sensors and we have shown how such sensors might be designed to maximize the linear operating region. In the present work, we will describe our efforts in actually designing and incorporating a spin-valve sensor into a gigabit-type shielded read head. We will then examine the magnetic and recording performance of these spin-valve recording heads.

II. SENSOR MATERIALS & DESIGN

Spin-valve films with the structure 50\AA Ta/ 100\AA NiFe/ 25\AA Cu/ 22\AA Co/ 110\AA FeMn were deposited by D.C. magnetron sputtering. The magnetic and spin-valve responses of the free layer along its easy-axis are characterized by low field measurements shown in Figs. 2a and 2b, respectively. Both responses exhibit hysteresis loops shifted from zero field. The shift corresponds to a

Best Available Copy

3802

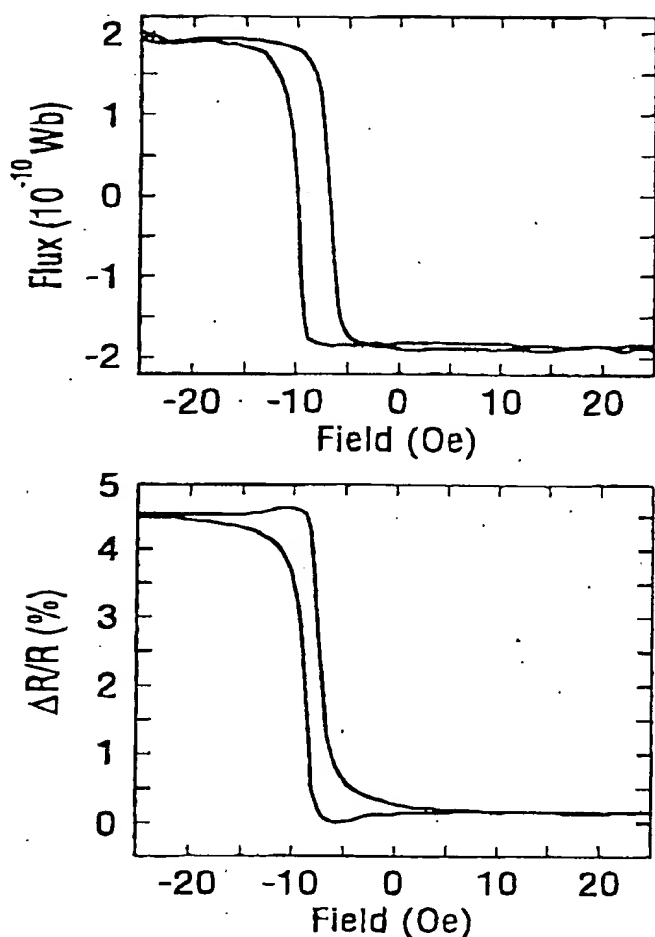


Fig. 2. Low field BH loop (a) and Spin-valve response (b) of the NiFe/Cu/Co/FeMn spin-valve sensor in as deposited films.

moderate ferromagnetic interlayer coupling field of 8 Oe, equivalent to a coupling energy of 5×10^{-3} ergs/cm². Fig. 2b also shows the spin-valve coefficient to be -4.6% and the easy-axis coercivity to be -1 Oe. Other measurements show the uniaxial anisotropy of the free layer to be 3 Oe, the sheet resistivity of the entire structure to be $15.5 \Omega/\square$, and the exchange-bias field of the Co/FeMn pinned layer to be as high as 400 Oe.

To optimize the linear operating region of the NiFe/Cu/Co spin-valve sensor, the thicknesses of the free and the pinned layers were determined by a micromagnetic modeling study of the sensor behavior in a shielded read head environment. As described in a previous work, this model uses as its inputs the resistivities, anisotropies, coupling fields and thicknesses of the pinned and the free magnetic layers as well as the height of the sensor. It then employs a finite element algorithm to determine the biasing profile and the transfer curve response to magnetic flux excitations as from transitions in recording. Results of our previous micromagnetic study show that the linear operating region of the transfer curve is maximized when

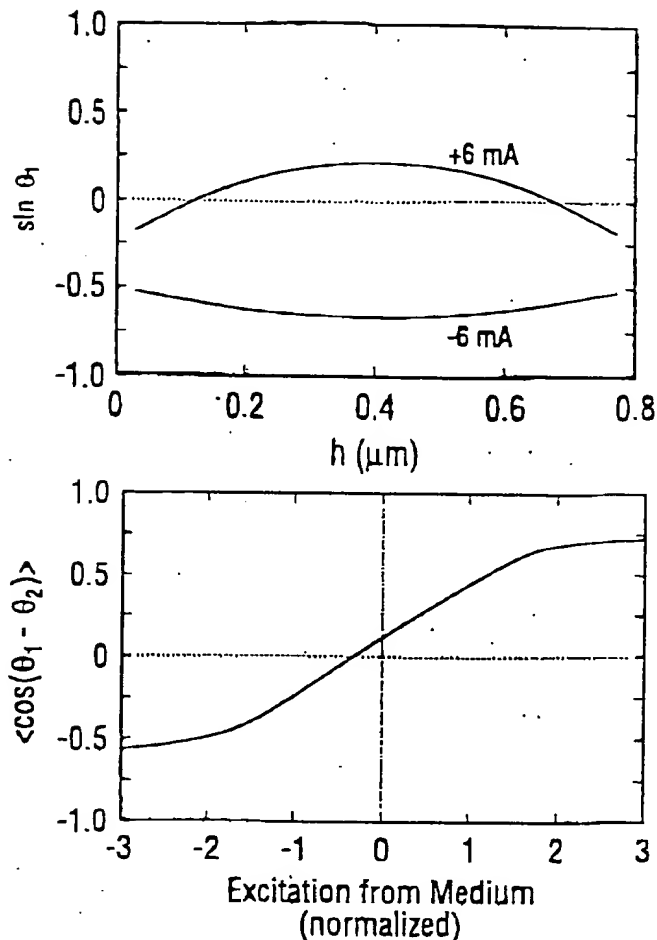


Fig. 3. Theoretical bias profile (a) and transfer curve (b) of the optimized sensor design (solid line: transfer curve; dotted line: derivative of transfer curve).

magnetostatic coupling between the pinned and the free layer, favoring antiparallel magnetic alignment, is on the whole balanced by the sum of the ferromagnetic interlayer coupling and the magnetic field of the sensor current [9]. Application of this modeling study to the present spin-valve system yields an optimum thickness combination of 100 Å for the NiFe free layer with 22 Å for the Co pinned layer. Fig. 3a shows the magnetic bias profile of the free layer for the optimized design. At a sensor current of +6 mA, the free layer magnetic moment is seen to be roughly longitudinal ($\theta_1 \approx 0$). The non-uniformity of the magnetostatic coupling effects, however, precludes its perfect cancellation by the ferromagnetic coupling and the current biasing effects, so that the free layer magnetic moment actually varies by up to $\pm 20^\circ$ (Fig. 3a) about the longitudinal direction along the height of the sensor. Fig. 3b shows the theoretical transfer curve of the optimized design, with a linear response region terminated at both ends by magnetic saturation effects. The quiescent state of the sensor is around the middle of the linear response region, yielding maximum signal dynamic range for linear operation.

Best Available Copy

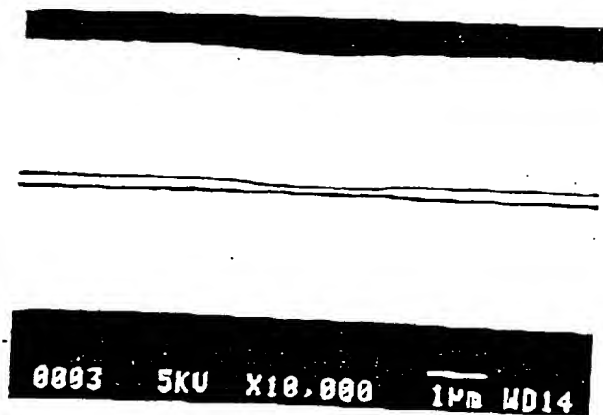


Fig. 4. SEM micrograph of spin-valve read head Air-Bearing Surface after lapping.

III. READ HEAD CONFIGURATION AND FABRICATION

The optimized spin-valve sensor, with characteristics described above, was incorporated into a shielded read head configuration similar to the gigabit recording head reported previously [13]. The sensor has a nominal read trackwidth of $2\mu\text{m}$, and is stabilized by longitudinal bias fields applied from the tail regions. The total read gap is $0.25\mu\text{m}$, with alumina as the gap material and $3\mu\text{m}$ thick electroplated permalloy layers as the shield material. The material deposition, lithography and patterning sequence for the spin-valve read head are similar to those employed for a standard MR read head. Thermal cycles in the fabrication process were found to result in a $\sim 20\%$ reduction in the spin-valve coefficient, yielding a final spin-valve coefficient of $\sim 3.5\%$ for the spin-valve read heads. After wafer fabrication, the read heads were mechanically lapped to a sensor stripe height of $\sim 1\mu\text{m}$. Fig. 4 shows the SEM micrograph of a spin-valve read head at the ABS (Air-Bearing Surface) after lapping to final stripe height.

IV. TRANSFER CURVE STUDY

After slider fabrication and suspension, the spin-valve recording heads were studied for their transfer curve behavior under external transverse magnetic field excitation. Fig. 5a and 5b show the low ($\pm 100\text{ Oe}$) and high ($\pm 350\text{ Oe}$) field transfer curves of a $2\mu\text{m}$ trackwidth spin-valve head at $\pm 6\text{ mA}$ sense current, which corresponds to a temperature rise of $\sim 25^\circ\text{C}$ above ambient. The transfer curves for the two opposite sense current polarities are indeed observed to be quite different, reflecting the different quiescent bias states as illustrated in Fig. 3a. For the present spin-valve sensors, the positive current is the design current direction. This is illustrated by the fact that one sense current polarity (bottom curves of Fig. 5) yields a large small-signal response amplitude (Fig. 5a) and a quiescent state fairly

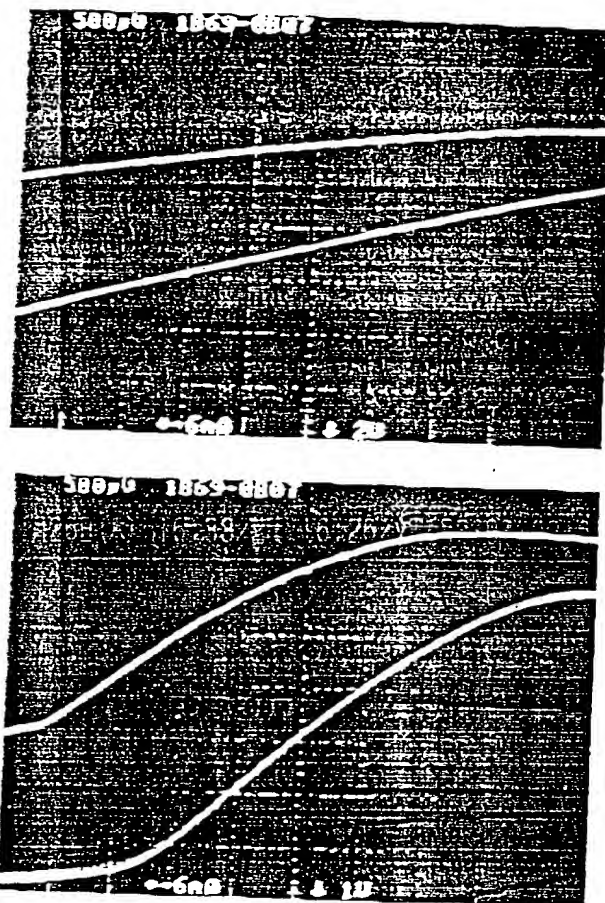


Fig. 5. Experimental low field ($\pm 100\text{ Oe}$) and high field ($\pm 350\text{ Oe}$) transfer curves of spin-valve read head.

close to the middle of the linear operating region (Fig. 5b). In contrast, the opposite sense-current polarity yields a low small-signal response amplitude and a quiescent bias state closer to magnetic saturation. Next, the high field transfer curves show a mild convexity in the linear operating region around zero field. This feature is somewhat unexpected from the linearity of the basic GMR behavior, and further analysis shows that it is probably caused by a small canting of the pinned layer's magnetic moment from the transverse direction. This canting reflects a misorientation of the Co/FeMn exchange bias direction during head processing, and can be seen to cause non-linearities in (i) by letting $\theta_2 = \pi/2$. Fig. 5a and 5b also show the GMR response of these narrow track spin-valve sensors to be quiet, stable and non-hysteretic for field excitations ($\pm 350\text{ Oe}$) strong enough to induce sensor saturation at the ABS. This result indicates that the application of a longitudinal bias field from the tail regions is as effective in inducing quiet and single-domain behavior in the spin-valve sensors as in the case of the conventional MR sensors.

BEST AVAILABLE COPY

3804

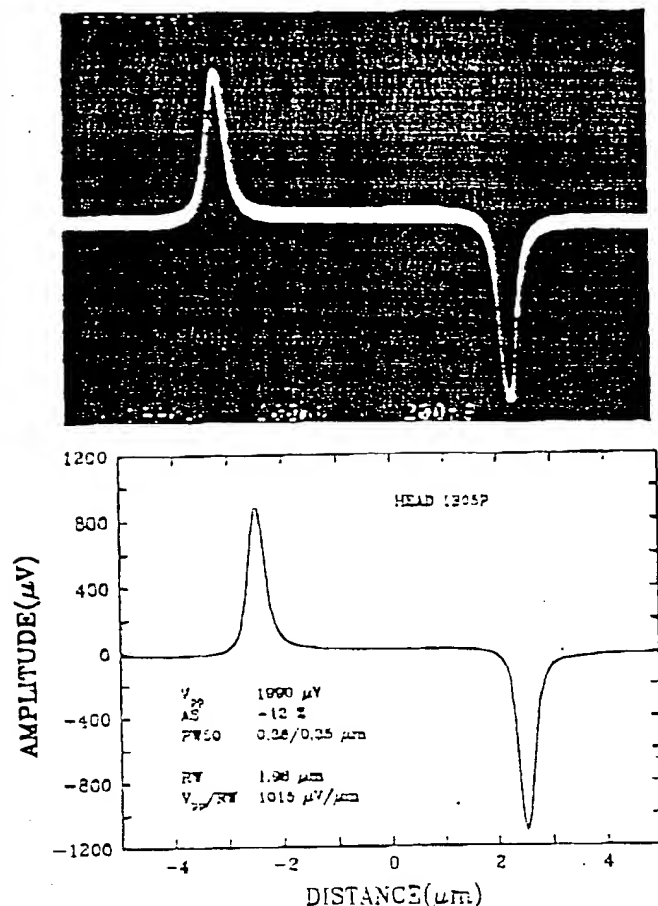


Fig. 6. Real-time (a) and Averaged (b) readback waveform of spin-valve head on CoCrPt disk.

V. RECORDING PERFORMANCE STUDY

The recording performance of these spin-valve read heads was tested on CoPtCr thin-film disks with an areal moment of as high as 1.25 memu/cm^2 , coercivity of 2500 Oe and coercive squareness of 0.8. The read heads were operated at currents corresponding to -25°C temperature rise above ambient, and they were flown at a clearance of $-1.5 \mu\text{m}$, corresponding to a total head-disk magnetic spacing of $-3.0 \mu\text{m}$. A separate write head is used for data writing. It has a relatively wide write trackwidth of $-5 \mu\text{m}$ to minimize read-write head misalignment effects.

Very large trackwidth normalized readback sensitivities of $750 \mu\text{V}/\mu\text{m}$ to $1000 \mu\text{V}/\mu\text{m}$ (peak-to-peak) were observed for these spin-valve heads. This sensitivity range is about a factor of three larger than that obtained in our previous gigabit experiment with conventional MR heads [13]. Fig. 6a and 6b show respectively the real-time and the averaged readback waveform for a $2 \mu\text{m}$ trackwidth spin-valve sensor. A peak-to-peak signal of $-2000 \mu\text{V}$ is achieved, with excellent signal-to-noise conditions free of magnetic instability or noise (Fig. 6a).

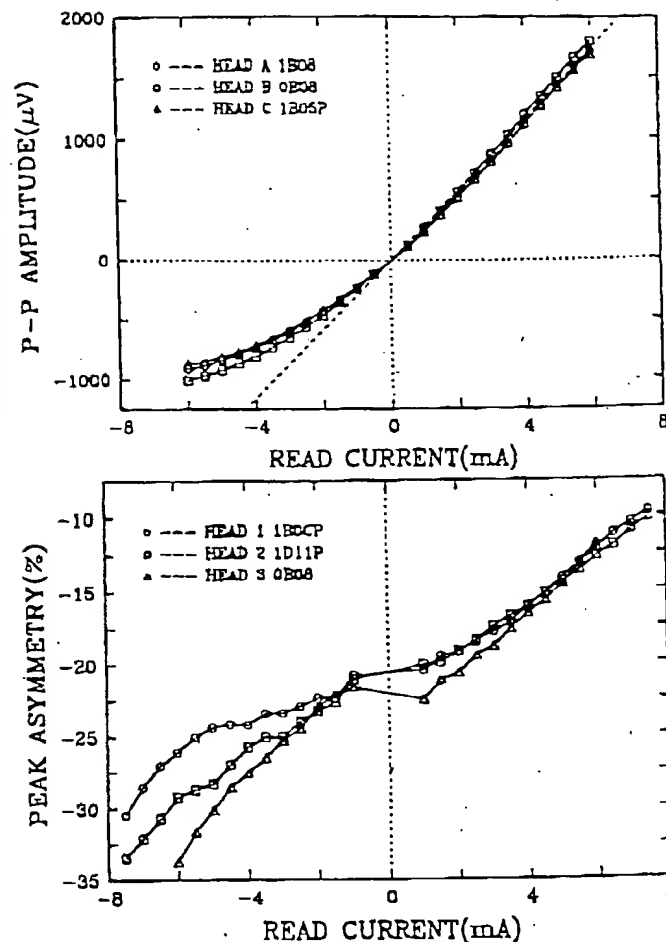


Fig. 7. Readback signal amplitude (a) and asymmetry (b) of spin-valve read heads vs. sensor current (Amplitude for negative current is plotted as negative for clarity; Asymmetry is difference over sum of the positive and negative signal peaks).

Fig. 6b shows both the positive and the negative sign responses to exhibit sharp peaks and similar half-width (PW50), revealing no sign of magnetic saturation despite the high areal moment of the recording media. The negative peak is, however, larger than the positive one, yielding a mild amplitude asymmetry of -10% . This amplitude asymmetry might be attributed to the slight transfer current convexity as discussed earlier. Next, the variation of a spin-valve head readback performance with sense current is studied by measuring the signal amplitude (Fig. 7a) and asymmetry (Fig. 7b) as a function of the sense current. Fig. 7a shows the signal amplitude to be roughly linear with sense current along the one current direction, but highly sub-linear along the other current direction, due to the movement of the quiescent bias state from the center of the linear operating region (Fig. 3b) towards magnetic saturation. This behavior is revealed even more clearly in Fig. 7b, where the amplitude asymmetries decrease rapidly and monotonically as the sense current varies from one direction to its opposite. These behaviors agree with expectations.

Best Available Copy

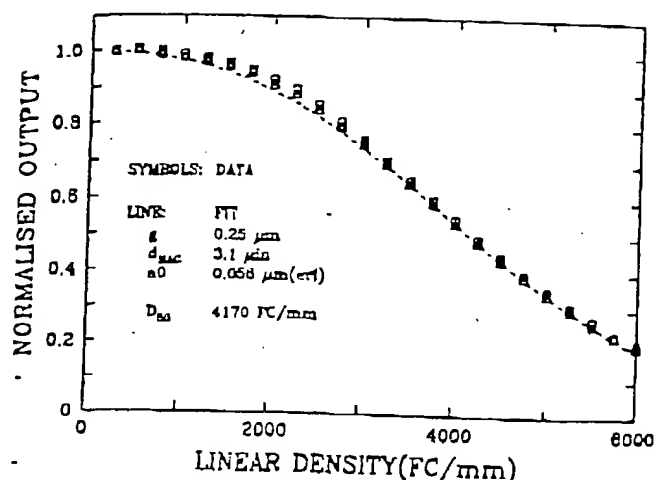


Fig. 8. Experimental and theoretical rolloff curves of the spin-valve read heads.

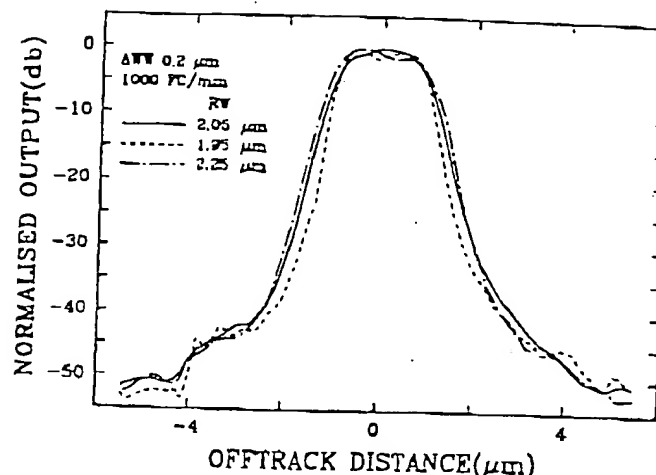


Fig. 9. Microtrack profiles of the spin-valve read heads.

from our micromagnetic modeling study, highlighting the importance of operating the spin-valve sensor only along the correct sense current direction.

Next, the linear and track density resolutions were studied. Fig. 8 shows the linear density rolloff behavior of three spin-valve heads. The signal amplitude decreases monotonically with linear density in a manner typical of the conventional MR sensors as well. To analyze the rolloff data, the transition width is estimated by the Williams-Cornstock model with error-function transition profiles, while the readback process is modeled by the reciprocity principle. Result shows good agreement between experimental and theoretical rolloffs at a total head-disk spacing of 3.1 μm , which is estimated from the flying conditions in our experiment. This agreement between the experiment and the linear readback model indicates that the spin-valve heads are not magnetically saturated even on disks with areal moments as high as 1.25 memu/cm². It confirms the large signal range capability for spin-valve sensors as expected when the free layer magnetic moment is along the longitudinal direction. The 50% rolloff densities are around 4200 fc/mm, which are toward the lower end of the rolloff densities as measured in the previous gigabit experiment [13]. This is mainly the result of broader transition profiles from a higher areal moment in the present recording media. To improve the linear resolution, therefore, some of the amplitude performance might be traded off by using a media with a lower areal moment (e.g., ~ 1 memu/cm²). A better approach is to redesign the spin-valve sensor with a thinner free layer so that it fits optimally with a lower areal moment media. Finally, the track resolution is studied by measuring the microtrack profile of the spin-valve heads. In this measurement, the data track is first reduced to $\sim 0.2 \mu\text{m}$ in trackwidth by erasure from the sides. The spin-valve head is then scanned over this microtrack while the signal at the fundamental data frequency is recorded. Results (Fig. 9) show well-behaving read head profiles with rapidly and monotonically decreasing signal amplitudes as the head moves offtrack. The profiles are also

symmetrical between the two opposite offtrack directions, due to the orientation of the free layer magnetic moment along the longitudinal 'unbiased' direction. This behavior is in distinct contrast to those for the conventional MR heads, which often exhibit pronounced left-right asymmetries as well as compensation point behaviors [13]. The halfwidths of the profiles yield read trackwidths around 2 μm , in agreement with the design target. The -30db widths of the profiles are only $\sim 4.5 \mu\text{m}$, much smaller than those for the conventional MR sensor in the previous gigabit experiment [13]. This reduction of side-reading is a result of several factors including the thinness of the free layer, the magnetic rigidity of the pinned layer as well as the 'unbiased' quiescent state of the free layer.

VI. CONCLUSIONS

We have successfully designed and fabricated NiFe/Cu/Co/FeMn spin-valve sensors in a gigabit type shielded read head configuration. Magnetic tests of the spin-valve heads with uniform fields reveal stable and quiet transfer curves with an optimally biased quiescent magnetic state. Small convexities in the overall transfer curves were detected and attributed to a small canting of the pinned layer magnetic moment from the ideal transverse direction. Recording tests of the spin-valve heads confirmed a large signal range capability due to the 'unbiased' nature of the quiescent magnetic state, resulting in no sensor saturation even with recording media of 1.25 memu/cm². Stable and quiet readback performance was observed, with signal amplitudes as large as 1000 $\mu\text{V}/\mu\text{m}$ at typical operating currents of around 6mA. Linear resolution studies showed satisfactory rolloff densities in good agreement with theory. Finally, track resolution studies showed the read trackwidths to agree with design target values, and read track profiles to be symmetrical and sharp, superior to the performance of conventional MR heads.

We are grateful to the many members in the Almaden Research Center and the Systems Storage Division who contributed to this effort. Technical support from J. S. Best and H. L. Hu are especially appreciated.

REFERENCES

- [1] M. Baibich, J. Broto, A. Fert, F. Nguyen Van Dau & F. Petroff, "Giant magnetoresistance of (001)Fe/(001)Cr magnetic superlattices," *Phys. Rev. Lett.*, 61(21), pp. 2472-2475, 1988.
- [2] B. Dieny, V. Speriosu, S. Metin, S. Parkin, B. Gurney, P. Baumgart & D. Wilhoit, "Magnetotransport properties of magnetically soft spin-valve structure," *J. Appl. Phys.*, 69(8), pp. 4774-4779, 1991.
- [3] B. Dieny, V. Speriosu, S. Parkin, B. Gurney, D. Wilhoit & D. Mauri, "Giant magnetoresistance in soft ferromagnetic multilayers," *Phys. Rev. B*, V 43, No. 1, pp. 1297-1300, 1991.
- [4] S. Parkin, "Dramatic enhancement of interlayer exchange coupling and giant magnetoresistance in $\text{Ni}_{81}\text{Fe}_{19}/\text{Cu}$ by addition of thin Co interface layers," *Appl. Phys. Lett.*, 61(11), pp. 1358-1360, 1991.
- [5] R. White, "Giant magnetoresistance: a primer," *IEEE Trans. Mag.*, MAG-28, No. 5, pp. 2482-2487, 1992.
- [6] J. Daughton, P. Bade, M. Jensen & M. Rahmati, "Giant magnetoresistance in narrow stripes," *IEEE Trans. Mag.*, MAG-28, No. 5, pp. 2488-2493, 1992.
- [7] A. Berkowitz, J. Mitchell, M. Corey & A. Young, "Giant magnetoresistance in heterogeneous Cu-Co alloys," *Phys. Rev. Lett.*, 68(25), pp. 3745-3748, 1992.
- [8] T. Hylton, K. Coffey, M. Parker & J. Howard, "Giant Magnetoresistance at low fields in discontinuous NiFe-Ag multilayer thin films," *Science*, 261, pp. 1021-1024, 1992.
- [9] D. Heim, R. Fontana, C. Tsang, V. Speriosu, B. Gurney & M. Williams, "Design and operation of spin valve sensors," *The Magnetic Recording Conference*, paper B5, 1993.
- [10] R. Hunt, "A Magnetoresistive Readout Transducer," *IEEE Mag Trans.*, MAG-7, No. 1, pp. 150-154, 1971.
- [11] D. Thompson, "Magnetoresistive transducers in high-density recording," *AIP Conf. Proc.*, 24, pp. 528-533, 1974.
- [12] C. Tsang, "A Theoretical Study of the Signal-response of a Shielded MR Sensor," *IEEE Trans. Magn.*, MAG-26, No. 6, pp. 3016-3021, 1990.
- [13] C. Tsang, M. Chen, T. Yogi & K. Ju, "Gigabit density recording using dual-element MR/Inductive heads on thin-film disks," *IEEE Trans. Mag.*, MAG-26, No. 5, pp. 1689-1693, 1990.

**This Page is Inserted by IFW Indexing and Scanning
Operations and is not part of the Official Record**

BEST AVAILABLE IMAGES

Defective images within this document are accurate representations of the original documents submitted by the applicant.

Defects in the images include but are not limited to the items checked:

- ☐ **BLACK BORDERS**
- ☐ **IMAGE CUT OFF AT TOP, BOTTOM OR SIDES**
- ☐ **FADED TEXT OR DRAWING**
- ☐ **BLURRED OR ILLEGIBLE TEXT OR DRAWING**
- ☐ **SKEWED/SLANTED IMAGES**
- ☐ **COLOR OR BLACK AND WHITE PHOTOGRAPHS**
- ☐ **GRAY SCALE DOCUMENTS**
- ☐ **LINES OR MARKS ON ORIGINAL DOCUMENT**
- ☐ **REFERENCE(S) OR EXHIBIT(S) SUBMITTED ARE POOR QUALITY**
- ☐ **OTHER:** _____

IMAGES ARE BEST AVAILABLE COPY.

As rescanning these documents will not correct the image problems checked, please do not report these problems to the IFW Image Problem Mailbox.